Aus der Hand-,Plastischen und Ästhetischen Chirurgie am

Klinikum der Ludwig-Maximilians-Universität München

Reliability and Comparison of 3-Dimensional Surface Imaging of the Face Using a Hand-Held and Whole body Surface Scanner

Dissertation

zum Erwerb des Doktorgrades der Medizin

an der Medizinischen Fakultät der

Ludwig-Maximilians-Universität München

vorgelegt von

Ya Xu

aus

Shangqiu,China

Jahr

2022

Mit Genehmigung der Medizinischen Fakultät der

Ludwig-Maximilians-Universität zu München

Erster Gutachter:	apl. Prof. Dr. med. Thilo Ludwig Schenck
Zweiter Gutachter:	Prof. Dr. Med. Riccardo Giunta
Dritter Gutachter:	Priv.-Doz. Dr. Dr. Florian Probst
Mitbetreuung durch den promovierten Mitarbeiter:	Dr. Med. Konstantin Frank Dr. Med. Konstantin Koban
Dekan:	Prof. Dr. med. Thomas Guderman
Tag der mündlichen Prüfung:	25.03.2022

Table of content

Zusammenfassung (Deutsch):

Ziel: Die dreidimensionale Oberflächenbildgebung (3DSI) hat sich als nützliches Werkzeug für plastische Chirurgen im präoperativen, intraoperativen und postoperativen Umfeld erwiesen. Nach Kenntnis der Autoren liegen keine Daten zur Reproduzierbarkeit und Genauigkeit der dreidimensionalen Oberflächenabbildung des Gesichts mit einem Ganzkörperscanner vor. Ziel dieser Untersuchung war es daher, die Reproduzierbarkeit von Gesichts-Scans zu bewerten, die mit Ganzkörper 3 – D Fotographie aufgenommen wurden, und die Präzision von Distanzmessungen im Gesicht zwischen einer portablen und einer stationären 3 – D Kamera zu vergleichen. Zudem wurde die Reproduzierbarkeit eines Ganzkörperscanners untersucht.

Material und Methoden: An dieser Untersuchung nahmen insgesamt 22 Probanden mit einem Durchschnittsalter von 29,36 Jahren teil. Zwei aufeinanderfolgende 3D-Bilder der Probanden wurden unter Verwendung einer Ganzkörper 3 – D Kamera (WB360) und einer portablen 3 – D Kamera (Vectra H2) erstellt. Es wurden bei jedem Scan Messungen vordefinierter Abstände im Gesicht durchgeführt und verglichen. Darüber hinaus wurde die Oberflächenabweichung zwischen zwei nacheinander erfassten Scans des Ganzköperscanners bewertet.

Ergebnisse: Für die Reproduzierbarkeit des Ganzkörper-Scans wurde der Abstand mit der geringsten statistischen Signifikanz mit p = 0.998 an der Nase gefunden, während die größte statistische Signifikanz mit p = 0.658 im Mittelgesicht gefunden wurde. Der Bereich mit der größten Oberflächenabweichung zwischen den überlagerten Scans war der Hals mit einem RMS von 1.62 ± 1.71 mm. Der Bereich mit der geringsten Oberflächenabweichung war die Stirn mit einem RMS von 0.17 ± 0.05. Für den Vergleich der beiden Scanner ergaben unsere Ergebnisse, dass sich der gemessene Unterschied zwischen der Länge und der Standardreferenz zwischen den beiden untersuchten Geräten in allen untersuchten Bereichen des Gesichts statistisch nicht signifikant unterschied (p > 0.266). Die gemessene Breite und die Breite der Standardreferenz unterschieden sich statistisch signifikant in allen Bereichen des Gesichts bei beiden untersuchten Geräten (p <0.032).

Schlussfolgerung: Das in dieser Studie untersuchte Ganzkörper 3 – D Kamera kann zur Erfassung des Gesichts verwendet werden und bietet eine ausreichende Genauigkeit für den Vergleich von Scans. Obwohl nicht direkt untersucht, kann angenommen werden, dass der Fehler, der durch die Neupositionierung des Patienten zwischen einer Basislinie und einem Follow-up-Scan verursacht wird, nicht zu groß ist, um Messungen, die mit dem Ganzkörper-Bildgebungsgerät durchgeführt wurden, als unpraktisch zu

betrachten. Sowohl die Messungen von Scans, die mit dem tragbaren Bildgebungsgerät als auch mit dem Ganzkörper-Bildgebungsgerät aufgenommen wurden, unterschieden sich signifikant von der Standardreferenz. Benutzer sollten sich der Abweichungen bewusst sein, wenn sie 3DSI mit den vorgestellten Bildgebungsgeräten erhalten, diese jedoch nicht unterlassen, da die absoluten Unterschiede möglicherweise zu gering sind, um sowohl in der klinischen als auch in der Forschung eine Rolle zu spielen.

Abstract (English):

Objective: 3-Dimensional surface (3DSI) imaging has been shown to be a useful tool for plastic surgeons in the preoperative, intraoperative and postoperative setting. And to the knowledge of the authors no data about the reproducibility and accuracy of 3-Dimensional surface imaging of the face using a whole-body scanner is available. Thus, the objective of this investigation was to assess the reproducibility of facial scans acquired using a whole-body imaging device and to compare the precision of distance measurements in the face using a hand-held surface imaging device and a whole-body surface imaging device. Furthermore, the reproducibility of the whole body scanner was investigated.

Material and Methods: This investigation enrolled a total of 22 healthy volunteers with a mean age of 29.36 years. Two consecutive 3-D images of the volunteers were obtained utilizing a whole-body imaging device(WB360) and a hand-hold imaging device(Vectra H2). For the whole-body imaging predefined distances in the face were performed in each scan and compared. Furthermore, surface deviation between two consecutively captured scans was assessed.

Results: For the reliability of whole-body scan, the distance with the smallest statistical significance was found to be at the nose with $p = 0.998$, while the biggest statistical significance was found in the midface with $p = 0.658$. The

area with the biggest surface deviation between the superimposed scans was the neck with a RMS of 1.62 ± 1.71 mm and the area with the smallest surface deviation was the forehead with a RMS of 0.17 ± 0.05 mm. For the comparison of the both scanners our results revealed that the measured difference between the length and the standard reference did not differ statistically significant between the two investigated devices in all investigated areas of the face ($p > 0.266$), however the measured difference of the width and the width of the standard reference differed statistically significant in all areas of the face across the investigated devices ($p < 0.032$).

Conclusion: The whole – body-imaging device investigated in this study can be utilized to capture the face and provides enough accuracy to compare scans. Even though not directly investigated, it can be hypothesized that the error caused by repositioning the patient between a baseline and a follow – up scan will not be too big to consider measurements performed with the whole – body-imaging device as impractical. Both, measurements obtained from scans acquired using the hand held imaging device and the whole – body-imaging device differed significantly from the standard reference. Users should be aware of deviations when obtaining 3DSI using the presented imaging devices but should not refrain from using them, as the absolute differences might be too small to play a role in both, clinical and research, setting.

List of figures

List of tables

List of abbreviations

3D	Three-Dimensional
3DSI	Three-Dimensional Surface Imaging
CT	Computerized tomography
MRI	Magnetic Resonance Imaging

1. Introduction

1.1 Preoperative evaluation

1.1.1 Preoperative plan and design

Preoperative evaluation is critical for surgical procedures. Preoperative assessment of a condition a patient presents with is critical do decide upon further treatment steps[1]–[4]. Preoperative assessment is also very important for plastic surgeons, as it can help them to have a profound influence on the choice of surgical methods[5], [6]. For example, in patients with breast reconstruction, we usually have two options, one is a breast reconstruction with implants, or use the rectus abdominal flap reconstruction[1], [6]–[9]. Accurate preoperative evaluation combined with the patient's wishes allows the plastic surgeon to make the best decision[4]–[6]. In addition, in ear reconstruction, accurate preoperative evaluation through 3D surface imaging can not only enable doctors to make a good surgical choice, but also provide a reliable basis for 3D printing of ear cartilage[10]–[12]. Preoperative planning can be considered as a roadmap leading to the desired result, in reconstructive, as well as in aesthetic plastic surgery[13]–[16]. The planning process needs to include the morphology of the patient’s body while at the same time characteristics of skin, soft tissue, sometimes even bone and allografts need to be considered[15],

[17]. A good clinical example for the necessity of doing a proper preoperative planning is the planning procedure of a mamma augmentation[15], [18]–[20]. The desired outcome of the patient needs to be discussed and the combination of the presenting morphology of the breast, tissue condition and implant choice need to be considered[1], [2], [6]–[8], [18]–[21].

Preoperative planning and design is a very important and challenging task for plastic surgeons. Due to the complex structure of human body surface, a good preoperative planning and design requires a high level of spatial thinking ability of plastic surgeons[4]–[6], [15]. Thalmaan attempted the first stereo photogrammetry of the face in 1944[13]. This was the first recorded attempt in the literature to use stereo photogrammetry in the clinical practice. This technique was based on photo measurements[22], [23]. The performed technique by Thalmaan was based on photo measurements. Thalmaan examined in his report an adult with facial asymmetry and an infant with Pierre - Robin syndrome[13]. An image of the object was taken from two different angles and then inserted into a plotter in order to draw a 3D contour map. This allowed for the first time to assess depth of a photograph in a quantitative way in medicine[22]–[24]. In 1967, Burke and Beard improved this technique by using simpler, cheaper cameras. They applied a multiplex plotting system to improve and shorten the time-consuming method of inserting a plotter on photographs. Their method was used to assess facial deformities in children

and to take facial measurements in the preoperative and postoperative setting[25]. In 1955, Ras et al. concluded that stereoscopic photogrammetry could quantify facial changes. These findings can be considered as the groundwork for the further development and clinical embedding of 3D imaging[23], [24], [26], [27]. In the following 20 years, with the continuous development of surface imaging technology, 3D surface imaging systems are now widely used in the medical field[1], [13], [21], [24], [28]–[33]. For example, before plastic surgery for breast reconstruction or breast implant surgery, accurate measurement of breast volume can be of valuable assistance to the surgeon[1], [6]–[9], [19]. The plastic surgeons can acquire information and be provided with further information to assess the symmetry of the breast and the necessary size of the used implant[1], [6], [7]. Prior to surgery of ear reconstruction in otolaryngology, 3D surface imaging of the contralateral ear can be used to facilitate the engraving of the rib cartilage graft during surgery[10]–[12], [34]. In dermatology, accurate 3D surface imaging of skin can assist dermatologists to judge the nature of nevi on the skin surface[4], [35]. With the introduction of 3D scanners in plastic surgery, preoperative planning and design of plastic surgery has become simpler and to some extent more accurate. Precise-enough preoperative imaging allows surgeons to get a good visual impression of the patient's complex statue. Using 3D imaging enables the plastic surgeon to appreciate potential deformities in a spatial manner.

Furthermore, 3D imaging can be used as a planning tool in plastic surgery. Proper planning using 3D imaging can aid the surgeon and might improve the success rate of patients[1], [13], [21], [24], [28]–[33], [35]–[38]. Another benefit of 3D imaging is the approximate visualization of anticipated changes to the patients. Simulation of changes utilizing 3D imaging, for example simulation of post - operative results after mamma – augmentation can facilitate the communication of a desired outcome between the surgeon and the patient[15], [18]–[20].

1.1.2 Comparison of 3D surface imaging and classical imaging modalities

Computer tomography, introduced in the literature in 1967 and magnetic resonance imaging, introduced in the literature in 1971, are classical imaging tools used in the daily practice of physicians[17], [39]. Both modalities allow for the visualization of internal structures of the body that are not visible to the physician. This change in radiological depiction of the human body has transformed the practice of medicine fundamentally[17], [39], [40]. However, computer tomography and magnetic resonance imaging are not only used to depict the internal body, however they also have been used to depict the surface of patients[17], [39]–[46]. As for the application of CT and MRI in surface imaging, most of them need to be combined with professional computer software for data processing[17], [39], [43]. For example, Mimics is an image

processing software developed by Belgium Materialise Co., Ltd. It has a history of more than 20 years and has become a professional medical image processing software[47]. The software can reconstruct CT/MRI and in 3D. Based on the 3D model, it can be applied to professional medical operations such as rapid medical model manufacturing, biological data analysis, implant design, and surgical process simulation through different modules[47], [48].

As a way to digitally record and consecutively depict the body, 3D surface imaging is cheap, easy to use and radiation – free. Especially compared to computer tomography, depiction of a body does not harm the patient as no harmful radiation is used[29]. Moreover, the resolution of the generated image does not depend on the dosage a patient is exposed to[17], [39], [47]. For example, in the preoperative estimation of breast volume, compared with MRI and 3D surface imaging, the cost of using 3D surface imaging is much lower[17], [39]. Of course, in terms of accuracy, as early as 10 years ago, Eder and Kovacs et al. had demonstrated that there is no significant difference between magnetic resonance imaging and 3D surface imaging in the calculation of breast volume[1]. For CT, the radiation-free aspect of 3D surface imaging is also a huge advantage, which not only eliminates patients' concerns about ionizing radiation, but also is relatively easy to use[29], [39]. It brings great convenience to preoperative, intraoperative and postoperative evaluation as 3D surface imaging can be conducted in an easy and handy manner. A possible

drawback of 3D surface imaging is the fact that it is not widely available and 3D surface imaging files cannot be sent out between physicians compared to sending out CT or MRI files[1], [13], [39].

1.1.3 Advantages of 3D imaging compared to traditional photography

Traditional photography has been used for many years as a two-dimensional evaluation method in plastic surgery in the preoperative, intraoperative and postoperative stage[23], [24], [49]–[51]. It is easy to learn, use and share, and visually evaluates the body or body part of patients. However, with the emergence of 3D surface imaging, the disadvantages of 2D photography have gradually emerged[31], [36], [52]. Classical 2 – Dimensional photography fails to provide accurate distance, volume and spatial measurements as it does not respect the 3 – Dimensional nature of the depicted body or body structure. This is mainly due to the lack of depth, which cannot be captured in a 2 – Dimensional photography[31][51]. Moreover, a plethora of point of views can be chosen when assessing a 3 – Dimensional photograph after the photo was taken. This is not possible in classical 2 – Dimensional photography[31], [36]. A disadvantage old 3D surface imaging is the fact that acquiring and taking a 3D photo requires a high level of expertise and requires cameras, which are expensive. Furthermore, the storage of the acquired 3D photos takes up much

more digital space than archiving classical images in the .jpg or .tiff format[24], [50].

1.1.4 Advantages of 3D imaging compared to traditional measurement methods

For traditional measurement methods, tapes, ruler, Vernier calipers and protractor are used to measure distances[38], [53]. Due to the influence of facial expressions and postures, it is inevitable that some human errors will be made in traditional methods[15], [53], [54]. Especially in the measurement of the skin surface, the traditional measurement method is often lacking reproducibility. In addition, traditional measurement methods are difficult to accurately measure the volume of the body or body parts[55], [56]. Compared to traditional measurement methods, 3D surface imaging allows to use standardizes measuring techniques that almost eliminate human errors and show a higher precision and reproducibility[28], [37], [57]. In addition, 3D surface imaging can accurately provide volume of the measured target, and is obviously superior to traditional measurement methods in morphological analysis such as symmetry[28], [37].

1.2 Intraoperative evaluation

In the intraoperative evaluation of plastic surgery, 3D surface imaging also plays a crucial role, especially in plastic and reconstructive surgery[6], [58]. One

example is the challenging reconstruction of a female breast using free tissue from the abdomen, called Deep Inferior Epigastric Perforator (DIEP) flap, following a complete breast resection (ablation) or total mastectomy[6]. Besides requiring a lot of experience and skill to perform such an operation, it is necessary to plan a free tissue transfer in detail, taking many factors into consideration such as the volume deficiency at the receiving site, former breast volume and surface ("breast footprint"), as well as an estimated overcorrection of the reconstructed breast compared to the healthy breast[58], [59]. In reconstructive breast surgery, there are several key steps in the intraoperative decision-making how to shape the form, symmetry, and volume of the reconstructed breast compared to the opposite site[60]–[62]. These decisions are made based mainly on the objective tape measurement, weighting or water-displacement measurement of specimens, and the subjective experience of the surgeon[62]–[64]. Therefore, if 3D surface imaging can bring some objective data analysis to doctors during intraoperative evaluation, it will be of great help to the successful completion of surgery[65]. With new hand-held scanners emerging since 2012, intraoperative measurement obstacles can be mastered systematically and current 3D mobile systems can meet precision requirements satisfactorily[66]. Another example of the intraoperative use of 3D imaging is a breast augmentation. By comparing the right and the left breast in terms of size,

height and shape can be assessed in an objective matter and yield a better postoperative results[6], [59]–[64], [67].

If used in a relatively fixed area, such as the operating room, it is difficult to move the stationary 3D scanner to the operating room. Hence using mobile, handheld 3D imaging device is the first choice. The disadvantage of these hand-held scanners is that the accuracy and resolution of the scanned images is not as high as that of a stationary scanner, but they are sufficient for clinical use.

1.3 Postoperative evaluation

3D surface imaging provides a new and practical method for the postoperative evaluation of plastic surgery[51], [68], [69]. It is well known that a patient's body shape changes slowly over time after plastic surgery. These changes mainly include changes in the morphology, location and volume of the surgical areas[13], [36], [51], [57]. After mamma augmentation and mastopexie, for example, there is a slight descend in the position and morphology of the breast, as a result of changes in the internal tissue of the operative area over time[50], [60], [63], [70]. In addition, after lipofilling on the breast and face, as the transferred fat is absorbed, and as the inflammation and swelling in the surgical area is reduced and the bleeding in the surgical area is absorbed, the volume of the surgical area will continuously change[59], [60], [65]–[67], [71]. The

monitoring of these changes relies on 3D surface imaging system, and data is processed in large quantities[72], [73]. Generated data can be used consecutively to anticipate changes in a more precise manner, which consecutively can be used to make planning more precise[68], [74]–[76]. In addition, using 3-D imaging the recovery process can be objectively monitored[77], [78]. In addition, for a few patients with poor postoperative results, the 3D surface imaging system can play a protective role for doctors when they are faced with law suits[79], [80]. Finally, with the passage of time and the increase of the number of follow-up visits, patients can clearly observe the healing of their wounds and the reduction of scar in each scan, which is of great help to some patients with postoperative anxiety[69], [80]–[83].

1.4 Imaging of the face

In facial 3D surface imaging, we can measure and analyze different facial indicators so as to quantify the surgical effect more objectively[28], [58]. Usually, the variables measured included distance, volume changes, and positional changes[84], [85]. For example, in blepharoplasties, the distance from eyelids to eyebrows can be measured before and after surgery to provide an objective reference for the surgical outcome[86]–[88]. In nasal reconstruction

surgery, we objectively quantify the effect by measuring the distance from the base of the nose to nasal tip and the distance from nasal root to nasal tip to tailor the necessary surgical steps. In lip surgery, the distance between the corners of the mouth is a better indication of the effect of the procedure[88]–[90]. After injection of HA – based fillers or autologous lipofilling, the amount of fillers or autologous fat can be planned through preoperative evaluation, and the changes in preoperative and postoperative volume can be evaluated through 3D surface imaging to help plastic surgeons judge the effect of interventions with quantitative indicators[5], [22], [87]–[89], [91], [92] . In Facelift procedures, positional changes can be assessed by 3D surface imaging processing. Not only can it help the plastic surgeon to make a better preoperative evaluation and planning, but it can also judge the effect of the surgery by combining the preoperative and postoperative facial morphology[23], [28], [55], [88]–[90], [92]–[96].

1.5 Common 3D imaging devices

The first stereo photogrammetry of the face has been reported in 1944[56], [69]. This was the first recorded attempt in the literature to use stereo photogrammetry in the clinical practice[56]. In 1967, Burke and Beard improved this technique by using simpler, cheaper cameras[25]. Over the next 50 years, a variety of 3D scanners have emerged[23], [32], [97]. Generally speaking, there

are two categories of 3 – D imaging systems[49], [57]. The first category is portable handheld 3D scanners, such as the Vectra H2 (Figure 1) (Canfield Scientific Inc., Parsippany, NJ, USA) or the Eva Artec (Artec 3D Inc., Luxembourg)[28], [58], [75], [89], [98]. These scanners are convenient, lightweight and low cost. If used in a relatively fixed area, such as the operating room, it is difficult to move the stationary 3D scanner to the operating room. Hence using mobile, handheld 3D imaging devices is the first choice. The disadvantage of these hand-held scanners is that the accuracy and resolution of the scanned images is not as high as that of a stationary scanner, but they are sufficient for clinical use[89], [99]–[103]. In addition, another disadvantage of handheld scanners is that the data needs to be temporarily stores on a U disk or laptop computer, which will bring some difficulties to the protection of the data, and the data may be exposed to potential risks of leakage and loss[104]–[107]. The second category is desktop scanners, such as Vectra XT (Canfield Scientific, Inc., Parsippany, NJ), Vectra360 (Canfield Scientific, Inc., Parsippany, NJ), etc. The Vectra XT is a stationary area scanner, which has a higher resolution and accuracy compared with handheld scanners. Furthermore it has its own independent database[103]–[107]. The drawback is that the Vectra XT is expensive compared to hand-held scans, and its lack of portability makes it difficult to use in specific environments, such as operating rooms or the ward. The main advantage of the Vectra WB360 is that it can scan the whole body

with extremely high resolution and accuracy. (Figure 2) This allows us to solve some of the problems in areas that are difficult to scan. The potential drawback for the Vectra 360 is that it is expensive and requires a large independent space to house it[32], [97], [99], [105]–[109].

Figure 1: Handheld 3D surface scanner H2 (Canfield Scientific Inc., Parsippany, NJ, USA).

Figure 2: Whole-body 3D surface scanner WB360 (Canfield Scientific, Inc., Parsippany, NJ).

1.6 Aim of this doctoral thesis

3–Dimensional surface (3DSI) imaging has been shown to be a useful tool for plastic surgeons in the preoperative, intraoperative and postoperative setting. To the knowledge of the authors no data about the reproducibility and accuracy of 3 – Dimensional surface imaging of the face using a whole-body scanner is available. Thus, the objective of this investigation was to compare the precision

of distance measurements in the face using a hand – held surface imaging device and a whole – body surface imaging device and to assess the reproducibility of facial scans acquired using a whole – body-imaging device.

2. Material and Methods

2.1 Study Sample

This investigation enrolled 22 healthy volunteer (12 Caucasian, 10 Asian) with a mean age of 29.36 ± 7.7 years and a mean BMI of 22.31 ± 1.5 kg/m^2. Participants were not enrolled in this study if previous facial surgeries, trauma, or diseases disrupted the integrity of the facial anatomy or major surface irregularities as tattoos or permanent make – up were present. Volunteers were taught on the methods and scopes of this investigation prior to enrolment. Volunteers were asked to sign a provided written informed consent for the use of their data and captured images prior to enrolment into the investigation. This investigation was reviewed and approved by the Institutional Review Board of Ludwig-Maximilian University Munich (IRB protocol number: 266-13). The study was performed in accordance with regional laws (Germany) and good clinical practice.

2.2 Imaging

3 – Dimensional surface images of the faces of the participants using a Vectra H2 hand - held camera system (Canfield Scientific Inc., Fairfield, New Jersey,

USA) and whole – body images using the WB360 system (Canfield Scientific Inc., Fairfield, New Jersey, USA) were captured.

Initially, participants were asked to step into the Vectra WB360 for the first image capture. After a period of 5 minutes, the second set of facial scans were captured for a second time using the WB360 to simulate a clinical setting. Upon completion, a standard reference in the form of a 6 mm x 38 mm Steri-Strip (3M Deutschland GmbH, Neuss, Germany) was placed on the forehead, on the midface (bilaterally) and on the lower face (in the midline) and 3 – Dimensional images of the participants were again captures using the Vectra H2 and WB360 scanner. (Figure 3)

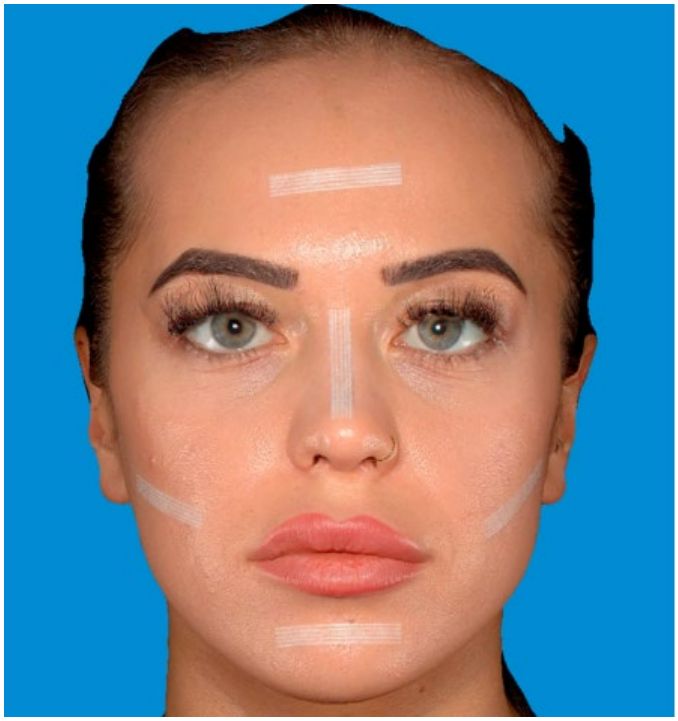

Figure 3: 3 – Dimensional surface image of a 25 – year old female participant with the attached steri – strips.

Volunteers were asked to stand upright with a resting, relaxed face. Participants were asked to maintain their facial expression over the duration of the image acquisition. Volunteers removed jewellery to allow for optimal imaging of the face. Upon completion of the acquisition of the photographs, scans were processed using the Vectra Software Suite® (Canfield Scientific Inc., Fairfield, New Jersey, USA).

2.3 Image Analyses

The 3 – Dimensional images were stitched automatically using the Vectra Software Suite® (Canfield Scientific Inc.). After stitching the following distance measurements were performed on scans of the WB360 (Figure 4):

P1 = Vertical distance between the upper margin of the eyebrow and the hairline as measured in the midpupillary line

P2= horizontal distance between the medial margins of their eyebrows

P3 = horizontal interpupillar distance

P4= vertical distance between the pupil and the ipsilateral oral commissure

P5 = vertical distance between P1 and the nasal tip in the midline

P6 = horizontal distance between the left and the right oral commissure

P7 = distance between the oral commissures and the mandibular symphysis

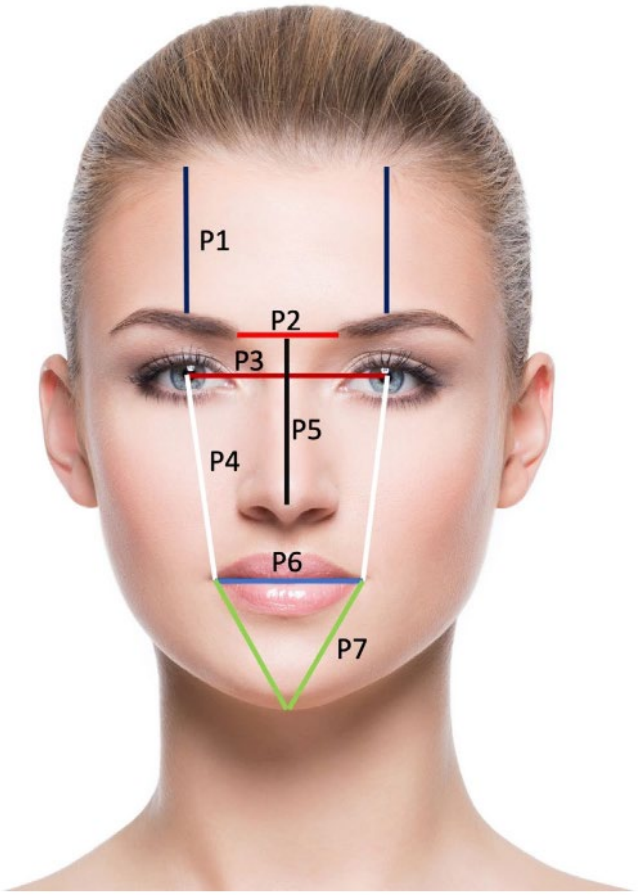

Figure 4: Figure showing the predefined measured distances.

Furthermore, to calculate the differences in surface projection between the baseline and each subsequent 3D scan, the surface – to – surface root-mean-square analysis and the iterative closest point (ICP) algorithm included in the Mirror Software Suite® (Canfield Scientific Inc.,) were performed. To perform this, an alignment of the initial and the consecutive scan captured with the WB360 was automatically performed to minimize investigator bias. The alignment is based on an software inherent algorithm. After automatic registry of the surface of the compared 3 – Dimensional photographs the given aesthetic

subunits were marked on the scans. Upon closure examination of the alignment of the scans a plethora of points are offset positively or negatively. As a mean of the distance of the offset of the points would probably cancel out each other (due to their positive and negative nature) and cause a mean divergence of about zero, surface – to – surface offsets are recorded by the squared mean. This root – mean – square analysis describes the squared mean to calculate the amount of surface offset. A perfect registry and alignment of the surfaces would thus create a value of 0 mm. Using the root – mean – square allows to weigh points with a greater offset in a greater proportion.

Areas of interest (Figure 5) were

- Forehead, defined as the area between a horizontal line at the level of the eyebrows and the beginning of the hair
- Peri – ocular region, defined as the area within the visible bony orbit
- Nose, defined as the area of the nose
- Cheek, defined as the medial and lateral midface, bordered by a line from the tragus along the periocular region up to the nose and along the jawline
- Perioral region, defined as the area of the oral commissure
- Mental region, defined as the area of the chin within the labiomental folds

- Neck, defined as the area from the mandible up to the clavicle

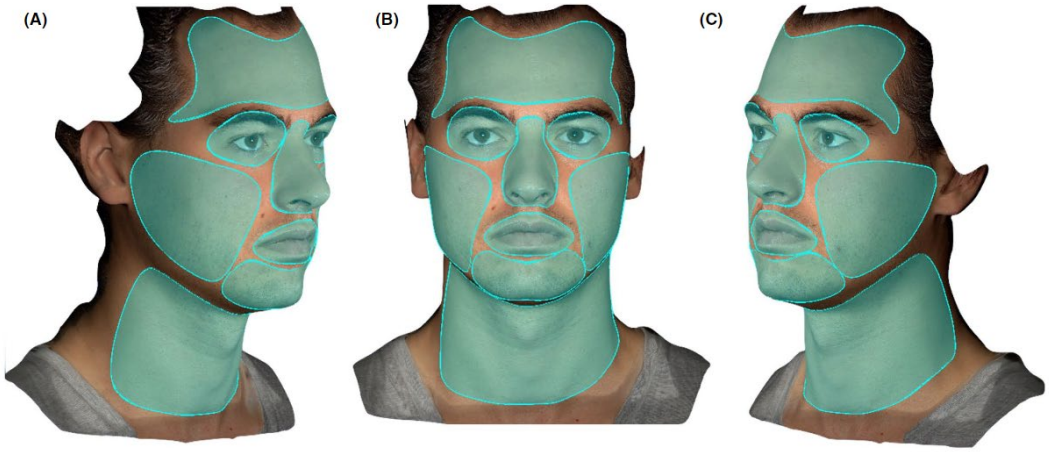

Figure 5: 3-dimensional surface imaging showing the respective aesthetic subunits used for the RMS analysis of a participant from right oblique (A), frontal (B), and left oblique (C)

Upon measuring the distances and RMS in the consecutively captured scans taken with the WB360, distance measurements of the applied steri – strips were performed for the second scans taken with the Vectra WB360 and Vectra H2. Following distance measurements were performed in each scan (Figure 3):

1) Length and width of the photographed steri – strip on the forehead
2) Length and width of the photographed steri – strip on the midface (bilaterally)
3) Length and width of the photographed steri – strip on the lower face

2.4 Statistical Analyse

2.4.1 Statistical Analyse (WB360)

Differences of the distance measurements between the two scans were calculated and compared using paired sample t-test for the respective same locations and compared using multi – variate analysis (ANOVA) for all investigated locations. All calculations were performed using SPSS Statistics 26 (IBM, Armonk, NY, USA) and results were considered statistically significant at a probability level of ≤ 0.05 to guide conclusions.

2.4.2 Statistical Analyse (WB360 vs. H2)

The difference to the length of the standard reference was calculated for each of the images obtained with the two investigated surface imaging devices (H2 vs. WB360) and compared via a paired student's t-test. Differences between the length and width of the standard reference and the measured length and width were calculated as relative and absolute values and compared using Student's T – test. Analyses were performed using SPSS Statistics 23 (IBM, Armonk, NY, USA) and differences were considered statistically significant at a probability level of $\leqslant$ 0.05 to guide conclusions.

3. Results

3.1 Results (WB360)

A total of 220 measurements were conducted in ten different regions of interest. The mean difference between the measurement in the first and the second scan was -0.13 ± 1.3 mm [Range: -4.06 – 5.34] independent of investigated location. The absolute average between the first and the second scan had a mean of 0.90 ± 0.90 mm [Range: 0.01 – 5.34]. Both, mean difference and mean absolute difference between the first and the second scan was statistically significantly different with $p < 0.001$. The distance with the smallest difference between the first and the second scan was the horizontal distance between the most medial point of the left eyebrow and the most medial point of the right eyebrow at the most inferior point of the eyebrow with 0.44 ± 0.28 mm, while the distance with the biggest difference was the straight distance over the surface between the most superior point of the eyebrow to the hairline with 1.28 ± 0.94 mm [Range: 0.03 – 4.06]. The RMS for the entire face was 0.44 ± 0.76 mm. The biggest RMS was observed at the neck with 1.62 ± 1.71 mm while the lowest RMS was observed at the forehead with 0.17 ± 0.05 mm. The RMS differed significantly across the investigated sub-units with $p < 0.001$.

3.1.1 Upper face measurements

P1 (= vertical distance between the upper margin of the eyebrow and the hairline as measured in the midpupillary line) measured on average 58.52 ± 13.1 mm in the first scan and of 59.41 ± 13.0 mm in the second scan (p = 0.751). P2 (horizontal distance between the medial margins of the eyebrows) measured 21.80 ± 4.4 mm in the first scan and at 21.62 ± 4.2 mm in the second scan (p = 0.886) on average. P3 (= horizontal interpupillar distance) measured on average 73.00 ± 4.9 mm in the first scan and at 72.99 ± 4.8 mm in the second scan with p = 0.992. Mean differences between the measurements of the upper face in the first and in the second scan are given in Table 1 .

Distance	Mean difference in mm ± SD	P – Value
P1	1.28 ± 0.94	0.751
P2	0.44 ± 0.28	0.886
P3	0.53 ± 0.68	0.992

Table 1: Table showing the mean difference in mm ± SD for P1, P2 and P3.

The RMS for the forehead was 0.17 ± 0.05 mm, while the RMS of the peri-ocular region was 0.41 ± 0.25 mm. The RMS of the areas in the upper face differed significantly with p < 0.001. (Table 2)

Investigated Subunit	RMS ± SD
Forehead	0.17± 0.05
Peri – ocular region	0.41± 0.25

Table 2: Table showing the RMS ± SD ob the investigated subunits in the upper face.

3.1.2 Midface measurements

P4 (vertical distance between the pupil and the ipsilateral oral commissure) measured 75.62 ± 4.0 mm in the first scan and 76.00 ± 4.0 mm in the second scan with p = 0.658. P5 (vertical distance between P1 and the nasal tip in the midline) measured 53.35 ± 4.0 mm in the first scan and 53.35 ± 4.0 mm in the second scan with p = 0.998. P6 (horizontal distance between the left and the right oral commissure) measured on average 61.05 ± 5.0 mm in the first scan and a mean of 60.77 ± 5.3 mm in the second scan with p = 0.862. Mean differences between the measurements of the midface in the first and in the second scan are given in Table 3.

Distance	Mean difference in mm ± SD	P – Value

P4	0.82 ± 0.77	0.658
P5	0.58 ± 0.48	0.998
P6	0.85 ± 0.89	0.862

Table 3: Table showing the mean difference in mm ± SD for P4, P5 and P6.

The RMS of the cheek region was 0.26 ± 0.09 mm, in the perioral region 0.36 ± 0.19 mm and at the nose 0.20 ± 0.06 mm. The RMS of the areas in the midface differed significantly with $p < 0.001$. (Table 4)

Investigated Subunit	RMS ± SD in mm
Nose	0.20 ± 0.06
Cheek	0.26 ± 0.10
Perioral	0.36 ± 0.19

Table 4: Table showing the RMS ± SD ob the investigated subunits in the midface.

3.1.3 Lower face measurements

P7 (distance between the oral commissures and the mandibular symphysis) measured on average 55.00 ± 3.9 mm in the first scan and 54.64 ± 3.97 mm in the second scan with p = 0.667. The RMS of the mental region was 0.24 ± 0.11 mm while the RMS of the neck was 1.62 ± 1.71 mm. The RMS of the areas in the lower face differed significantly with p = 0.001. (Table 5)

Investigated Subunit	RMS ± SD in mm
Mental Region	0.24 ± 0.11
Neck	1.62 ± 1.71

Table 5: Table showing the RMS ± SD ob the investigated subunits in the lower face.

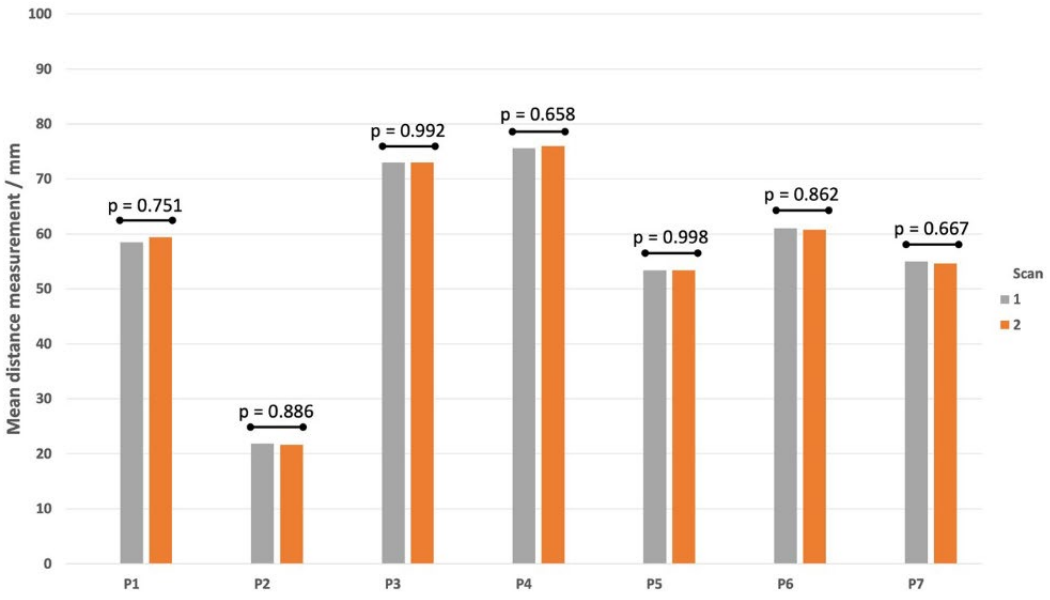

Figure 6: Bar graph showing the distance measurements in the first scan and the second scan for P1 and P7 with the respective p - values.

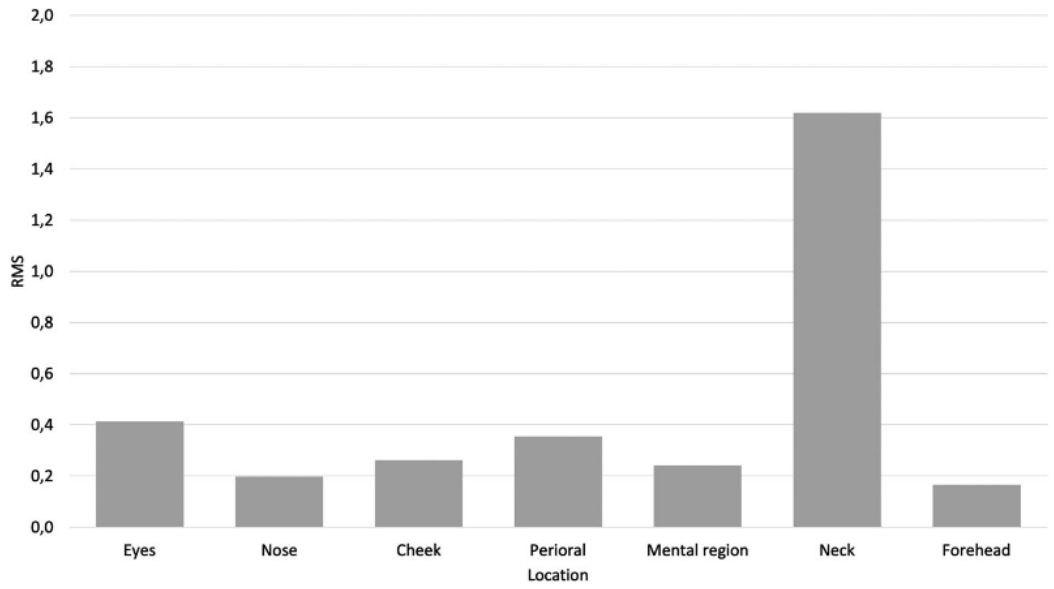

Figure 7: Bar graph showing the mean Root mean square for the respective aesthetic subunits.

3.2 Results (WB360 vs H2)

The average difference between the length and width of the standard reference and the measured length and width, independent of investigated facial area (forehead vs. midface vs. lower face vs. nose) or investigated surface imaging device was -0.56 ± 0.9 mm and 0.33 ± 0.2 mm respectively. Independent of facial region, the mean difference to the standard reference of the measured length was -0.65 ± 0.8 mm for the H2 imaging device and -0.46 ± 1.0 mm for the WB360 imaging device with p = 0.112. Independent of facial region, the mean difference to the standard reference of the measured width was 0.29 ± 0.1 mm for the H2 imaging device and 0.37 ± 0.3 mm for the WB360 imaging device with p = 0.017. A significant difference between the differences across

the different investigated areas of the face was found for measured lengths and widths ($p < 0.001$).

3.2.1 Forehead measurements

The average difference between length of the standard reference and the measured length in the forehead was -0.29 ± 0.3 mm for the H2 and -0.40 + 0.5 mm for the WB360 ($p = 0.422$). The average difference between width of the standard reference and the measured width was 0.32 ± 0.2 mm for the H2 and 0.43 + 0.2 mm for the WB360 ($p = 0.032$). Paired samples T-test revealed a significant difference between the length of the standard reference and the measured length for both, the H2 and the WB360 with $p = 0.001$ and $p = 0.002$ respectively, and between the width of the standard reference and the measured width $p < 0.001$ for both, H2 and WB360. (Figure 8, 9, 10, 11 and Table 6, 7, 8, 9)

3.2.2 Midface measurement

The average difference between length of the standard reference and the measured length in the midface was -0.35 ± 0.4 mm for the H2 and -0.21 + 0.7 mm for the WB360 ($p = 0.266$). The average difference between width of the standard reference and the measured width was 0.28 ± 0.2 mm for the H2 and 0.50 + 0.2 mm for the WB360 ($p < 0.001$). Paired samples T-test revealed a

significant difference between the length of the standard reference and the measured length for both, the H2 and the WB360 with $p < 0.001$ and $p = 0.048$ respectively, and between the width of the standard reference and the measured width $p < 0.001$ for both, H2 and WB360. (Figure 8, 9, 10, 11 and Table 6, 7, 8, 9)

Lower face measurements

The average difference between length of the standard reference and the measured length in the lower face was -1.80 ± 1.0 mm for the H2 and -1.68 + 1.1 mm for the WB360 ($p = 0.718$). The average difference between width of the standard reference and the measured width was 0.28 ± 0.1 mm for the H2 and 0.43 + 0.1 mm for the WB360 ($p < 0.001$). Paired samples T-test revealed a significant difference between the length of the standard reference and the measured length for both, the H2 and the WB360 with $p < 0.001$, and between the width of the standard reference and the measured width $p < 0.001$ for the H2 and WB360. (Figure 8, 9, 10, 11 and Table 6, 7, 8, 9)

Forehead		Midface		Lower Face	
H2	WB360	H2	WB360	H2	WB360
0.29 ± 0.4	0.40 ± 0.5	0.35 ± 0.4	0.21 ± 0.7	1.80 ± 1.0	1.68 ± 1.1
p = 0.422		p = 0.266		p = 0.718	

Table 6: Table depicting the mean difference between length of the standard reference and the measured length in mm for the respective location and the respective imaging device. P – values for the difference between the respective imaging devices are given.

Forehead		Midface		Lower Face	
H2	WB360	H2	WB360	H2	WB360
-0.32 ± 0.2	-0.43 ± 0.2	-0.28 ± 0.2	-0.50 ± 0.2	-0.28 ± 0.1	-0.43 ± 0.1
p = 0.032		p < 0.001		p < 0.001	

Table 7: Table depicting the mean difference between width of the standard reference and the measured length in mm for the respective location and the respective imaging device. P – values for the difference between the respective imaging devices are given.

Forehead		Midface		Lower Face	
H2	WB360	H2	WB360	H2	WB360
p = 0.001	p = 0.002	p < 0.001	p = 0.048	p < 0.001	p < 0.001

Table 8: Table depicting the p – values for differences between the length of the standard reference and the measured length.

Forehead		Midface		Lower Face	
H2	WB360	H2	WB360	H2	WB360
p < 0.001	p < 0.001	p < 0.001	p < 0.001	p < 0.001	p < 0.001

Table 9: Table depicting the p – values for differences between the width of the standard reference and the measured width.

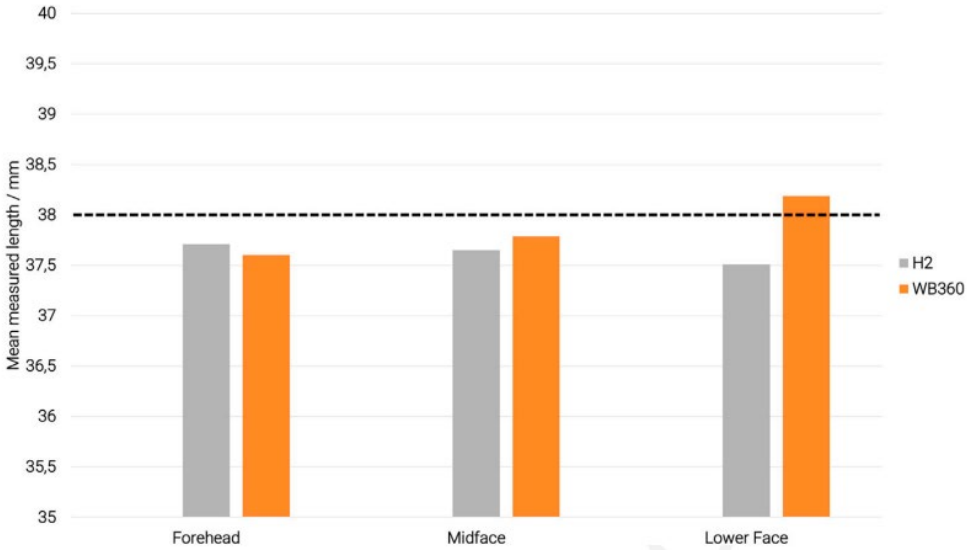

Figure 8: Bar chart showing the mean measured length in mm for the forehead, midface, and lower face for the H2 and WB360.

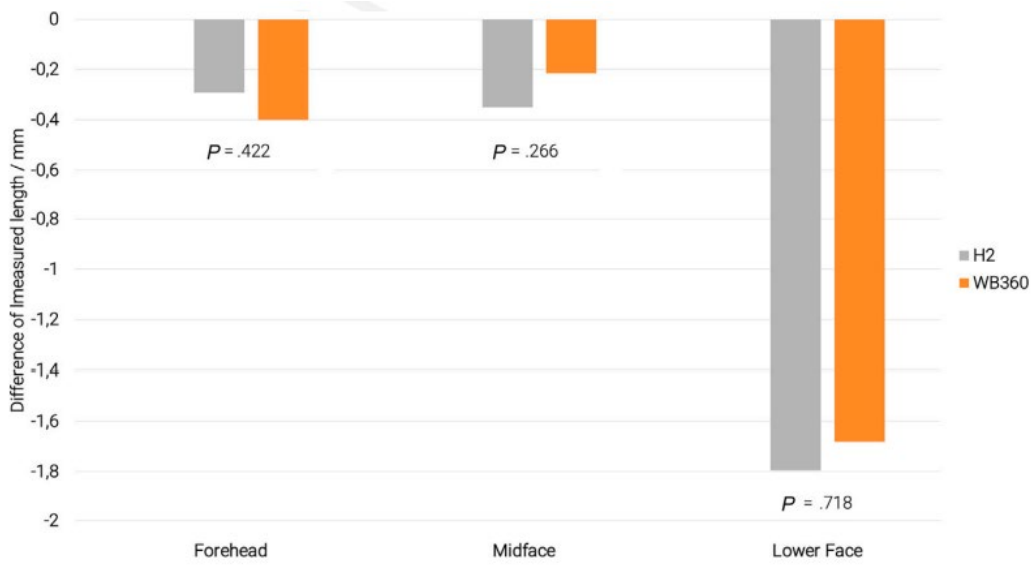

Figure 9: Bar chart showing the average difference between the length of the standard reference and the measured length for the H2 and WB360. P – values between the 2 camera systems are given.

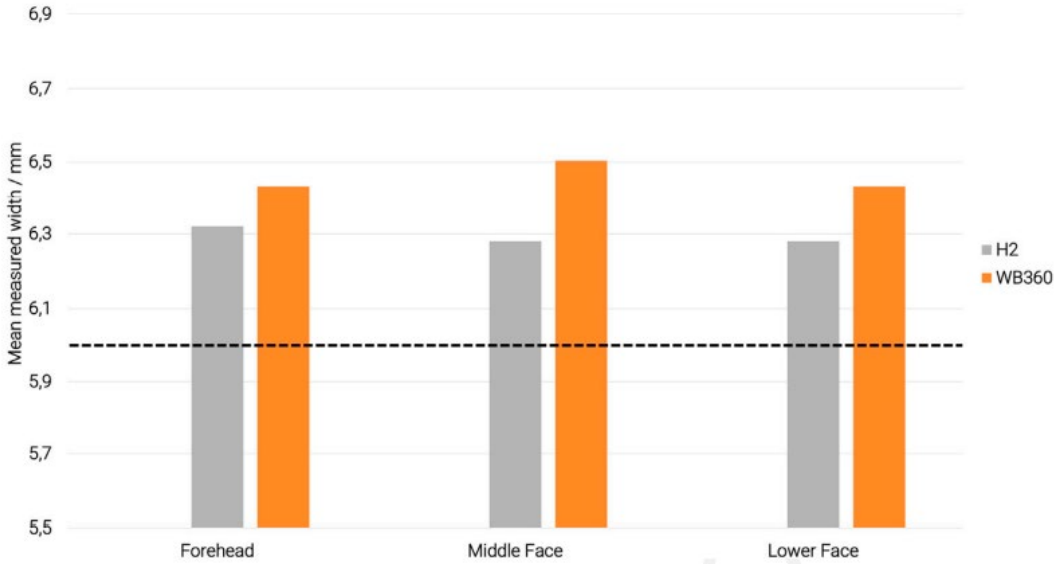

Figure 10: Bar chart showing the mean measured width in mm for the forehead, midface, and lower face for the H2 and WB360, respectively.

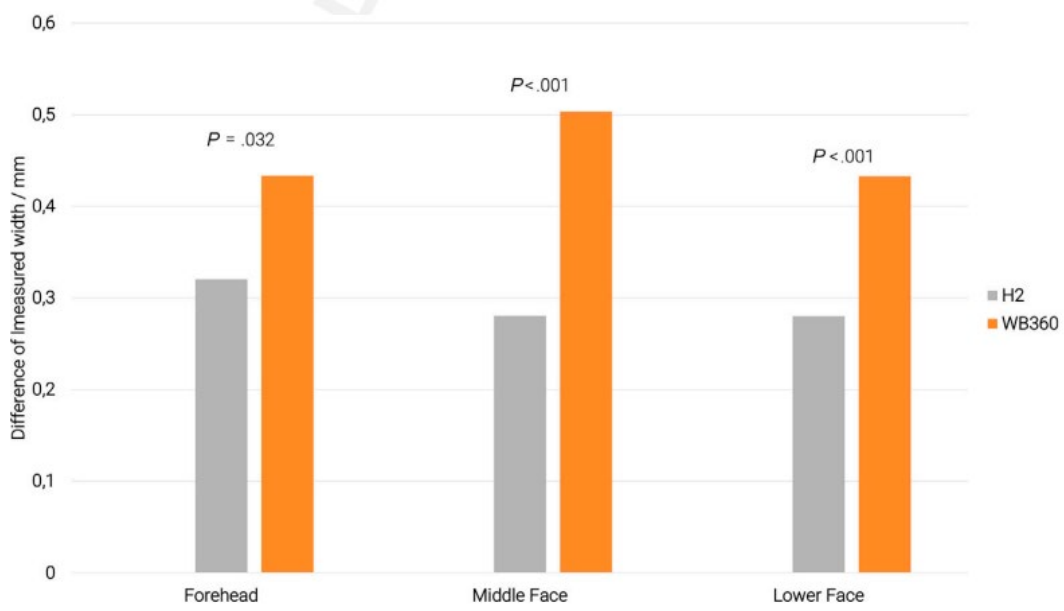

Figure 11: Bar chart showing the average difference between the width of the standard reference and the measured width for the H2 and WB360.

4. Discussion

4.1 Reliability of 3 – Dimensional Surface Imaging of the Face using a whole body surface scanner

One aim of this study is to investigate the reliability of facial imaging using a whole – body surface imaging device (WB360) by comparing standardized distance measurements of two consecutively created face – scans and by assessing the surface deviation of the two consecutively captured images. A total of 220 distance measurements in 22 participants were conducted. The distance with the smallest statistical significance was between the distance measurements at the intersection between the horizontal distance between the most medial point of the left eyebrow and the most medial point of the right eyebrow at the most inferior point of the eyebrow and the nasal tip in the midline with $p = 0.998$. The biggest statistical significance was found for the straight distance over the surface between the midpupil to the corner of the mouth with $p = 0.658$. The area with the biggest surface deviation between the superimposed scans was the neck with a RMS of 1.62 ± 1.71 mm and the area with the smallest surface deviation was the forehead with a RMS of 0.17 ± 0.05 mm.

A strength of this study was the standardized testing environment. Subjects were photographed in the same room with identical lighting. Due to the nature of the WB360, the position of the cameras remains steady which minimizes deviations from the technical side of the imaging process. All participants were scanned by the same investigator (Y.X.) who furthermore possesses longstanding experience with 3-Dimensional surface imaging. Moreover, all measurements were performed by the same investigator (Y.X.) which provides further consistency, as investigator-based inconsistency and error is minimized. By asking patients to remove jewelry and hair from their face, remain in the same position during the capturing of the two images and by capturing the images immediately after each other distracting movements which might alter the image acquisition process were minimized. In total, 220 measurements and RMS – calculations of 22 pairs of scans were performed. To the knowledge of the authors this is the biggest sample size in the literature that was investigated to validate measurements of a whole body 3-Dimensional surface imaging device.

A potential draw – back of the investigation is its limited clinical application. 3-D surface imaging is an important follow-up tool for researchers and clinicians; however patients will most likely not be able to occupy the same position at a follow-up scan as at the initial base-line scan. Participants of this investigation were captured immediately in sequence. This will be, as pointed out, barely

possible in the “real – life” setting and possibly contribute to bigger deviations. Additional factors, such as day – dependent swelling for example, may further affect image deviance. However, it can be assumed that those regions where we observed a bigger deviation will be more likely to remain areas of higher inaccuracy. Another potential limitation of this investigation is the bare measurement of distance – measurements. Especially in minimally – invasive procedures in the face assessing small volumetric changes that might have a huge impact on the perception of the face are important to capture. However, volumetric changes require invasive procedures, i.e., the injection of soft-tissue fillers into the participants face. Due to ethical concerns and the participants being volunteers rather than patients that asked for minimally invasive treatments as soft – tissue filler augmentations this investigation did not look at volumetric changes.

The findings of this investigation are in line with previous investigations that assessed the accuracy of 3 – D surface imaging devices to depict the face in the intraoperative setting. Koban et al. showed that the forehead is a region with small surface – deviation when comparing two scans, while eyes and the perioral region showed high surface – deviations[58]. A potential explanation for the high surface – deviation for the perioral region (0.36 ± 0.19) and the eyes (0.41 ± 0.25) might be the high mobility of those regions. The perioral and periocular region can be considered as the areas of the highest mobility in the

face, which is plausible as most of the verbal and non-verbal communication is conveyed by those regions. Even in our study setting, minimal – even unconscious – movements or involuntary contractions of the orbicularis oculi or orbicularis oris muscle might affect the surface state and consecutively measurements in this region. Physicians and researchers should keep in mind that those areas are thus susceptible for errors. Especially oculoplastic – surgeons should be reminded that comparisons of measurements that are performed within the ocular region need to be considered with caution and might lead to wrongfully interpreted results in the post-operative follow-up. Moreover, with the emergence of minimally – invasive treatments in the perioral region to enhance lips and the consecutive demand for scientifically based clinical studies that rely on 3 – D surface imaging to assess volumetric and spatial changes, again, measurements in this region should be considered with caution. A noteworthy result of our investigation was the exceptionally high RMS for the neck. Even though the investigated whole – body surface imaging device aims to depict the entire body, capturing surfaces that are horizontally aligned might be difficult for the WB360 as the cameras are pointing at the neck, especially the upper neck, from an oblique angle. Furthermore, the neck was the biggest aesthetic subunit that was investigated, which might furthermore add to the higher RMS.

Even though sources of error were minimized by capturing the images in series and evaluation by the same investigator inaccuracies between the two scans could be revealed. However, the measured distance did not differ in any instance significantly between the first and the second scan. We thus consider the investigated whole – body imaging device capable of capturing the face with enough accuracy for the clinical and research setting.

4.2 Comparison of 3 – Dimensional Surface Imaging of the Face using a Hand - held and Whole Body Surface Scanner

Another aim of this study is to investigate the accuracy of 3DSI scans obtained with a hand – held imaging device (Vectra H2) and a whole – body imaging device (WB360) by comparing the measurements obtained from the scans to a standard reference, which was a 38 x 6 mm sized steri – strip attached to various regions in the face of 22 individuals. Our results revealed that the measured difference between the length and the standard reference did not differ statistically significant between the two investigated devices in all investigated areas of the face ($p > 0.266$), however the measured difference of the width and the width of the standard reference differed statistically significant in all areas of the face ($p < 0.032$). When testing for statistical significance, the obtained measurements (both length and width) from the 3DSI scans differed

significantly from the standard reference in all areas of the face for both imaging devices (H2 and WB360) with $p \leq 0.048$.

A strength of this study is the constant testing environment. Images of the subjects were photographed under the same lighting conditions. Furthermore, due to capturing the images with both devices immediately after each other influences as altered mimic, local swelling or movement artefacts could be excluded. As all data was obtained by the same investigator (Y.X.) consistency could be provided and observer – dependent bias could be reduced. Furthermore, using standard references allowed to assess objectively whether the obtained measurements from the 3DSI over- or underestimated the respective lengths and widths. Furthermore, a sample size of 22 participants with five applied standard references yielded 98 observations, which is to the knowledge of the authors the biggest sample size that was investigated to validate and compare measurements of a hand-held and whole body 3DSI device. A potential drawback of this study is the standard reference itself. Even though steri – strips were not manipulated and checked with a calliper, this study relied on the manufacturers details about length and width of the produced steri – strips. The calliper measurements used did not show any difference between the stated size, however even if proper attachment was performed in all instances, minimal crimpling of the steri-strip, which might affect the measurement results, could not be excluded. Furthermore, adhesion of the

steri-strips might differ in-between the image capturing with the H2 and the WB360 due to transpiration of the individual. Another potential draw – back of this investigation is the lack of capturing volumetric changes. Especially in the follow – up of treatments with soft – tissue, fillers or autologous lipofilling volumetric changes are important. Our study did not include any volumetric changes, which might limit the clinical application of its findings, however the authors have the strong view that also spatial distance measurements are of inevitable importance in the clinical and research field.

Interestingly, the measurements of the length of the standard reference were most accurate in the midface when captured with the WB360 and least accurate in the lower face when captured with the H2. A possible explanation for this might be the diminished cohesivity of the steri – strips on the hairy lower face of males, which might consecutively caused the steri – strip to be off standing and minimally overlapping. Physicians should thus keep in mind that facial hair might disrupt the integrity and precision of a 3DSI scan and furthermore limit its evaluability. This finding is in line with recent findings by Koban et al. that found the greatest variation within scans to be at the mouth and the eye region[58].

Another finding of this investigation is that the measured length of the steri-strips was in general greater, while the measured width of the steri-strips was in average smaller. Practitioners should thus keep in mind that vertical

measurements might be underestimated when using both 3DSI devices, while horizontal measurements might likely be overstated.

The measured difference between length of the standard reference and the measured length was greater for the H2 than for the WB360 except at the forehead. This can be attributed to the creation of the image. The WB360 captures the face with 92 fixed installed cameras and the only source of error, i.e. changes in the face of the scanned individual, are caused by movement of the individual itself. Capturing a 3DSI with the H2 requires the investigator to take a face capture at a 45° angle from the front toward the right side of the face at the patient's chest level, directly in front of the face at the level of the patient's face not angled and at a 45° angle from the front toward the left side of the face at the patient's chest level. Simultaneously, two red dots need to be converged to allow for the optimal focus of the images taken. Even when painstakingly aiming to reproduce the same distances and angles this process is a source for human error in the capturing process. Additional to the aforementioned human error in the capturing process on the investigator's side, the same movement artefacts caused by the captured participant add to possible deviations. Practitioners should be aware, that using hand-held 3DSI devices adds a further source or error to the capturing process, compared to stationary 3DSI devices.

Even though p – values for differences between the length and width of the standard reference and the measured length and width were statistically highly significant in all investigated areas it needs to be pointed out that the absolute difference ranged from -1.14 to 4.3 mm. While statistically significant different, the divergence from the standard reference should still be considered acceptable. Clinical follow – up and follow – up imaging sessions in the research field require precise acquisition, however the – though statistically significant – deviations should be considered as acceptable.

5. Conclusion

The whole – body imaging device investigated in this study can be utilized to capture the face and provides enough accuracy to compare scans. Even though not directly investigated, it can be hypothesized that the error caused by repositioning the patient between a baseline and a follow – up scan will not be too big to consider measurements performed with the whole – body-imaging device as impractical.

Both, measurements obtained from scans acquired using the hand held imaging device and the whole – body imaging device differed significantly from the standard reference. However, the absolute differences were small. We thus conclude that physicians and researchers should be aware of deviations when obtaining 3DSI using the presented imaging devices but should not refrain from using them, as the absolute differences might be too small to play a role in both, clinical and research, setting.

References

[1] K. Chen *et al.*, “Preoperative breast volume evaluation of one-stage immediate breast reconstruction using three-dimensional surface imaging and a printed mold,” *J. Chinese Med. Assoc.*, vol. 82, no. 9, pp. 732–739, 2019, doi: 10.1097/JCMA.0000000000000155.

[2] H. Y. Choi, M. Park, M. Seo, E. Song, S. Y. Shin, and Y. M. Sohn, “Preoperative axillary lymph node evaluation in breast cancer: Current issues and literature review,” *Ultrasound Q.*, vol. 33, no. 1, pp. 6–14, 2017, doi: 10.1097/RUQ.0000000000000277.

[3] S. L. Cohn and L. Goldman, “Preoperative risk evaluation and perioperative management of patients with coronary artery disease,” *Med. Clin. North Am.*, vol. 87, no. 1, pp. 111–136, 2003, doi: 10.1016/S0025-7125(02)00143-8.

[4] M. E. Bilgili, H. Yildiz, B. P. Cengiz, and I. M. Saydam, “Effect of preoperative evaluation by a dermatologist on diagnostic accuracy,” *Dermatologic Surg.*, vol. 40, no. 12, pp. 1402–1408, 2014, doi: 10.1097/DSS.0000000000000168.

[5] O. Topsakal *et al.*, “Digitizing rhinoplasty: a web application with three-dimensional preoperative evaluation to assist rhinoplasty surgeons with surgical planning,” *Int. J. Comput. Assist. Radiol. Surg.*, vol. 15, no. 11, pp. 1941–1950, 2020, doi: 10.1007/s11548-020-02251-7.

[6] J. W. Kwong *et al.*, “Assessing the Accuracy of a 3-Dimensional Surface Imaging System in Breast Volume Estimation,” *Ann. Plast. Surg.*, vol. 84, no. 5S Suppl 4, pp. S311–S317, 2020, doi: 10.1097/SAP.0000000000002244.

[7] R. P. Ter Louw and M. Y. Nahabedian, “Prepectoral breast reconstruction,” *Plast. Reconstr. Surg.*, vol. 140, no. 5S, pp. 51S-59S, 2017, doi: 10.1097/PRS.0000000000003942.

[8] A. Y. Ho, Z. I. Hu, B. J. Mehrara, and E. G. Wilkins, “Radiotherapy in the setting of breast reconstruction: types, techniques, and timing,” *Lancet Oncol.*, vol. 18, no. 12, pp. e742–e753, 2017, doi: 10.1016/S1470-2045(17)30617-4.

[9] A. Homsy, E. Rüegg, D. Montandon, G. Vlastos, A. Modarressi, and B. Pittet, “Breast Reconstruction: A Century of Controversies and Progress,” *Ann. Plast. Surg.*, vol. 80, no. 4, pp. 457–463, 2018, doi: 10.1097/SAP.0000000000001312.

[10] Y. Tahiri and J. Reinisch, “Porous Polyethylene Ear Reconstruction,” *Clin. Plast. Surg.*, vol. 46, no. 2, pp. 223–230, 2019, doi: 10.1016/j.cps.2018.11.006.

[11] A. Sayan, T. E. Seah, and V. Ilankovan, “Reconstruction of a marginal defect of the ear: ‘another feather in the cap,’” *Br. J. Oral Maxillofac. Surg.*, vol. 57, no. 4, pp. 378–380, 2019, doi: 10.1016/j.bjoms.2019.02.011.

[12] Z. Tian-Yu and N. Bulstrode, “International consensus recommendations on microtia, aural atresia and functional ear reconstruction,” *J. Int. Adv. Otol.*, vol. 15, no. 2, pp. 204–208, 2019, doi: 10.5152/iao.2019.7383.

[13] B. Mailey *et al.*, “Evaluation of Facial Volume Changes after Rejuvenation Surgery Using a 3-Dimensional Camera,” *Aesthetic Surg. J.*, vol. 36, no. 4, pp. 379–387, 2016, doi: 10.1093/asj/sjv226.

[14] V. Veer, L. Jackson, N. Kara, and M. Hawthorne, “Pre-operative considerations in aesthetic facial surgery,” *J. Laryngol. Otol.*, vol. 128, no. 1, pp. 22–28, 2014, doi: 10.1017/S0022215113003162.

[15] J. Georgii *et al.*, “A computational tool for preoperative breast augmentation planning in aesthetic plastic surgery,” *IEEE J. Biomed. Heal. Informatics*, vol. 18, no. 3, pp. 907–919, 2014, doi: 10.1109/JBHI.2013.2285308.

[16] J. J. Elist, L. Levine, R. Wang, and S. K. Wilson, “Patient selection protocol for the Penuma® implant: suggested preoperative evaluation for aesthetic surgery of the penis,” *Int. J. Impot. Res.*, vol. 32, no. 2, pp. 149–152, 2020, doi: 10.1038/s41443-020-0237-5.

[17] N. J. Mankovich, D. R. Robertson, and A. M. Cheeseman, “Three-dimensional image display in medicine,” *J. Digit. Imaging*, vol. 3, no. 2, pp. 69–80, 1990, doi: 10.1007/BF03170565.

[18] M. A. Spring, E. C. Hartmann, and W. Grant Stevens, “Strategies and Challenges in Simultaneous Augmentation Mastopexy,” *Clin. Plast. Surg.*, vol. 42, no. 4, pp. 505–518, 2015, doi: 10.1016/j.cps.2015.06.008.

[19] L. A. Green, J. A. Karow, J. E. Toman, A. Lostumbo, and K. Xie, “Review of breast augmentation and reconstruction for the radiologist with emphasis on MRI,” *Clin. Imaging*, vol. 47, pp. 101–117, 2018, doi: 10.1016/j.clinimag.2017.08.007.

[20] P. E. Chasan, “Reductive Augmentation of the Breast,” *Aesthetic Plast. Surg.*, vol. 42, no. 3, pp. 662–671, 2018, doi: 10.1007/s00266-017-1010-0.

[21] M. Eder, A. Schneider, A. Zimmermann, and N. A. Papadopulos, “Brustvolumenbestimmung anhand der 3-D- Oberfla ¨ chengeometrie : Verifizierung der Methode mit Hilfe der Kernspintomographie Breast volume assessment based on 3D surface geometry : verification of the method using MR imaging,” pp. 112–121, 2008, doi: 10.1515/BMT.2008.017.

[22] J. Chen *et al.*, “Association between the Use of Social Media and Photograph Editing Applications, Self-esteem, and Cosmetic Surgery Acceptance,” *JAMA Facial Plast. Surg.*, vol. 21, no. 5, pp. 361–367, 2019, doi: 10.1001/jamafacial.2019.0328.

[23] L. Supit and T. O. H. Prasetyono, “A portable mirror stand for clinical facial photo documentation,” *Arch. Plast. Surg.*, vol. 42, no. 3, pp. 356–360, 2015, doi: 10.5999/aps.2015.42.3.356.

[24] C. H. J. Tzou and M. Frey, “Evolution of 3D Surface Imaging Systems in Facial Plastic Surgery,” *Facial Plast. Surg. Clin. North Am.*, vol. 19, no. 4, pp. 591–602, 2011, doi: 10.1016/j.fsc.2011.07.003.

[25] H. Ainsworth and M. Joseph, “An assessment of a stereophotogrammetric technique for the study of facial morphology in the child,” *Ann. Hum. Biol.*, vol. 3, no. 5, pp. 475–488, 1976, doi: 10.1080/03014467600001741.

[26] M. Eulitz and G. Reiss, “3D reconstruction of SEM images by use of optical photogrammetry software,” *J. Struct. Biol.*, vol. 191, no. 2, pp. 190–196, 2015, doi: 10.1016/j.jsb.2015.06.010.

[27] A. H. Tyson, G. E. Mawdsley, and M. J. Yaffe, “Measurement of compressed breast thickness by optical stereoscopic photogrammetry,” *Med. Phys.*, vol. 36, no. 2, pp. 569–576, 2009, doi: 10.1118/1.3065066.

[28] L. Kovacs *et al.*, “Accuracy and precision of the three-dimensional assessment of the facial surface using a 3-D laser scanner,” *IEEE Trans. Med. Imaging*, vol. 25, no. 6, pp. 742–754, 2006, doi: 10.1109/TMI.2006.873624.

[29] S. Fahrni *et al.*, “CT-scan vs . 3D surface scanning of a skull : first considerations regarding reproducibility issues,” *Forensic Sci. Res.*, vol. 2, no. 2, pp. 93–99, 2017, doi: 10.1080/20961790.2017.1334353.

[30] Y. Li, X. Yang, and D. Li, “The application of three-dimensional surface imaging system in plastic and reconstructive surgery,” *Ann. Plast. Surg.*, vol. 77, no. 00, pp. S76–S83, 2016, doi: 10.1097/SAP.0000000000000813.

[31] S. Nitkunanantharajah, G. Zahnd, M. Olivo, N. Navab, P. Mohajerani, and V. Ntziachristos, “Skin Surface Detection in 3D Optoacoustic Mesoscopy Based on Dynamic Programming,” *IEEE Trans. Med. Imaging*, vol. 39, no. 2, pp. 458–467, 2020, doi: 10.1109/TMI.2019.2928393.

[32] R. Imran and T. L. Rogers, “Resolving Reflection and Resolution in 3D Imaging of Fresh Bone,” *J. Forensic Sci.*, vol. 65, no. 1, pp. 200–208, 2020, doi: 10.1111/1556-4029.14136.

[33] K. Lee, M. Kim, and K. Kim, “3D skin surface reconstruction from a single image by merging global curvature and local texture using the guided filtering for 3D haptic palpation,” *Ski. Res. Technol.*, vol. 24, no. 4, pp. 672–685, 2018, doi: 10.1111/srt.12584.

[34] A. Olshinka, M. Louis, and T. A. Truong, “Autologous Ear Reconstruction,” *Semin. Plast. Surg.*, vol. 31, no. 3, pp. 146–151, 2017, doi: 10.1055/s-0037-1603959.

[35] S. Abadie *et al.*, “3D imaging of cleared human skin biopsies using light-sheet microscopy: A new way to visualize in-depth skin structure,” *Ski. Res. Technol.*, vol. 24, no. 2, pp. 294–303, 2018, doi: 10.1111/srt.12429.

[36] Y. Knafo, F. Houfani, B. Zaharia, F. Egrise, I. Clerc-Urmès, and D. Mainard, “Value of 3D Preoperative Planning for Primary Total Hip Arthroplasty Based on Biplanar Weightbearing Radiographs,” *Biomed Res. Int.*, vol. 2019, 2019, doi: 10.1155/2019/1932191.

[37] A. M. Mahmoud, P. Ngan, R. Crout, and O. M. Mukdadi, “High-resolution 3d ultrasound jawbone surface imaging for diagnosis of periodontal bony defects: An in vitro study,” *Ann. Biomed. Eng.*, vol. 38, no. 11, pp. 3409–3422, 2010, doi: 10.1007/s10439-010-0089-0.

[38] J. Marotz *et al.*, “3D-perfusion analysis of burn wounds using hyperspectral imaging,” *Burns*, vol. 47, no. 1, pp. 157–170, 2021, doi: 10.1016/j.burns.2020.06.001.

[39] S. Li, D. Liu, G. Yin, P. Zhuang, and J. Geng, “Real-time 3D-surface-guided head refixation useful for fractionated stereotactic radiotherapy,” *Med. Phys.*, vol. 33, no. 2, pp. 492–503, 2006, doi: 10.1118/1.2150778.

[40] B. A. Foex and A. Russell, “BET 2: CT versus MRI for occult hip fractures,” *Emerg. Med. J.*, vol. 35, no. 10, pp. 645–647, 2018, doi: 10.1136/emermed-2018-208093.3.

[41] J. Buchholz, E. Ludewig, A. Brühschwein, D. Nitzl, A. Sumova, and B. Kaser-Hotz, “Radiation therapy planning using MRI-CT fusion in dogs and cats with brain tumors,” *Tierarztl. Prax. Ausgabe K Kleintiere - Heimtiere*, vol. 47, no. 1, pp. 5–12, 2019, doi: 10.1055/a-0806-6366.

[42] A. Gallastegui, E. Davies, A. L. Zwingenberger, S. Nykamp, M. Rishniw, and P. J. Johnson, “MRI has limited agreement with CT in the evaluation of vertebral fractures of the canine trauma patient,” *Vet. Radiol. Ultrasound*, vol. 60, no. 5, pp. 533–542, 2019, doi: 10.1111/vru.12785.

[43] P. S. N. Van Rossum *et al.*, “Imaging of oesophageal cancer with FDG-PET/CT and MRI,” *Clin. Radiol.*, vol. 70, no. 1, pp. 81–95, 2015, doi: 10.1016/j.crad.2014.07.017.

[44] Z. Hu *et al.*, “From PET/CT to PET/MRI: Advances in instrumentation and clinical applications,” *Mol. Pharm.*, vol. 11, no. 11, pp. 3798–3809, 2014, doi: 10.1021/mp500321h.

[45] K. M. Hasebroock and N. J. Serkova, “Toxicity of MRI and CT contrast agents,” *Expert Opin. Drug Metab. Toxicol.*, vol. 5, no. 4, pp. 403–416, 2009, doi: 10.1517/17425250902873796.

[46] O. Ohana, S. Soffer, E. Zimlichman, and E. Klang, “Overuse of CT and MRI in paediatric emergency departments,” *Br. J. Radiol.*, vol. 91, no. 1085, 2018, doi: 10.1259/bjr.20170434.

[47] C. Aktuna Belgin, M. Colak, O. Adiguzel, Z. Akkus, and K. Orhan, “Three-dimensional evaluation of maxillary sinus volume in different age and sex groups using CBCT,” *Eur. Arch. Oto-Rhino-Laryngology*, vol. 0, no. 0, p. 0, 2019, doi: 10.1007/s00405-019-05383-y.

[48] A. Nayak, P. K. Jain, P. K. Kankar, and N. Jain, “Computer-aided design–based guided endodontic: A novel approach for root canal access cavity preparation,” *Proc. Inst. Mech. Eng. Part H J. Eng. Med.*, vol. 232, no. 8, pp. 787–795, 2018, doi: 10.1177/0954411918788104.

[49] W. Zhang, D. A. Kosiorek, and A. N. Brodeur, “Application of Structured-Light 3-D Scanning to the Documentation of Plastic Fingerprint Impressions: A Quality Comparison with Traditional Photography,” *J. Forensic Sci.*, vol. 65, no. 3, pp. 784–790, 2020, doi: 10.1111/1556-4029.14249.

[50] J. M. Weissler, C. S. Stern, J. E. Schreiber, B. Amirlak, and O. M. Tepper, “The Evolution of Photography and Three-Dimensional Imaging in Plastic Surgery,” *Plast. Reconstr. Surg.*, vol. 139, no. 3, pp. 761–769, 2017, doi: 10.1097/PRS.0000000000003146.

[51] G. M. Galdino, D. DaSilva, and J. P. Gunter, “Digital photography for rhinoplasty,” *Plastic and Reconstructive Surgery*, vol. 109, no. 4. pp. 1421–1434, 2002, doi: 10.1097/00006534-200204010-00035.

[52] L. B. Jørgensen *et al.*, “Validation of three-dimensional wound measurements using a novel 3D-WAM camera,” *Wound Repair Regen.*, vol. 26, no. 6, pp. 456–462, 2018, doi: 10.1111/wrr.12664.

[53] D. Wang, H. Liu, and X. Cheng, “A miniature binocular endoscope with local feature matching and stereo matching for 3d measurement and 3d reconstruction,” *Sensors (Switzerland)*, vol. 18, no. 7, 2018, doi: 10.3390/s18072243.

[54] J. S. Wheat, S. Clarkson, S. W. Flint, C. Simpson, and D. R. Broom, “The use of consumer depth cameras for 3D surface imaging of people with obesity: A feasibility study,” *Obes. Res. Clin. Pract.*, vol. 12, no. 6, pp. 528–533, 2018, doi: 10.1016/j.orcp.2018.05.001.

[55] K. P. Lincoln, A. Y. T. Sun, T. J. Prihoda, and A. J. Sutton, “Comparative Accuracy of Facial Models Fabricated Using Traditional and 3D Imaging Techniques,” *J. Prosthodont.*, vol. 25, no. 3, pp. 207–215, 2016, doi: 10.1111/jopr.12358.

[56] S. M. Weinberg, “3D stereophotogrammetry versus traditional craniofacial anthropometry: Comparing measurements from the 3D facial norms database to Farkas’s North American norms,” *Am. J. Orthod. Dentofac. Orthop.*, vol. 155, no. 5, pp. 693–701, 2019, doi: 10.1016/j.ajodo.2018.06.018.

[57] L. Kovacs *et al.*, “New aspects of breast volume measurement using 3-dimensional surface imaging,” *Ann. Plast. Surg.*, vol. 57, no. 6, pp. 602–610, 2006, doi: 10.1097/01.sap.0000235455.21775.6a.

[58] K. C. Koban, P. Perko, L. Etzel, Z. Li, T. L. Schenck, and R. E. Giunta, “Validation of two handheld devices against a non-portable three-dimensional surface scanner and assessment of potential use for intraoperative facial imaging,” *J. Plast. Reconstr. Aesthetic Surg.*, vol. 73, no. 1, pp. 141–148, 2020, doi: 10.1016/j.bjps.2019.07.008.

[59] N. Beisemann *et al.*, “Intraoperative 3D imaging leads to substantial revision rate in management of tibial plateau fractures in 559 cases,” *J. Orthop. Surg. Res.*, vol. 14, no. 1, p. 236, 2019, doi: 10.1186/s13018-019-1286-7.

[60] S. R. Yarboro, P. H. Richter, and D. M. Kahler, “Die Entwicklung der 3-D-Bildgebung in der Versorgung orthopädischer Verletzungen,” *Unfallchirurg*, vol. 120, no. 1, pp. 5–9, 2017, doi: 10.1007/s00113-016-0226-9.

[61] P. Paul, O. Fleig, and P. Jannin, “Augmented virtuality based on stereoscopic reconstruction in multimodal image-guided neurosurgery: Methods and performance evaluation,” *IEEE Trans. Med. Imaging*, vol. 24, no. 11, pp. 1500–1511, 2005, doi: 10.1109/TMI.2005.857029.

[62] A. Elmi-Terander *et al.*, “Pedicle Screw Placement Using Augmented Reality Surgical Navigation with Intraoperative 3D Imaging: A First In-

Human Prospective Cohort Study," *Spine (Phila. Pa. 1976).*, vol. 44, no. 7, pp. 517–525, 2019, doi: 10.1097/BRS.0000000000002876.

[63] D. Hammerle, G. Osterhoff, F. Allemann, and C. M. L. Werner, "Comparison of intraoperative 2D vs. 3D imaging in open reduction and fixation of distal radius fractures," *Eur. J. Trauma Emerg. Surg.*, vol. 46, no. 3, pp. 557–563, 2020, doi: 10.1007/s00068-018-1036-2.

[64] I. S. Alam *et al.*, "Emerging Intraoperative Imaging Modalities to Improve Surgical Precision," *Mol. Imaging Biol.*, vol. 20, no. 5, pp. 705–715, 2018, doi: 10.1007/s11307-018-1227-6.

[65] F. Wilde, K. Lorenz, A. K. Ebner, O. Krauss, F. Mascha, and A. Schramm, "Intraoperative imaging with a 3D C-arm system after zygomatico-orbital complex fracture reduction," *J. Oral Maxillofac. Surg.*, vol. 71, no. 5, pp. 894–910, 2013, doi: 10.1016/j.joms.2012.10.031.

[66] M. Schnetzke *et al.*, "Intraoperative 3D imaging in the treatment of elbow fractures - A retrospective analysis of indications, intraoperative revision rates, and implications in 36 cases," *BMC Med. Imaging*, vol. 16, no. 1, pp. 4–11, 2016, doi: 10.1186/s12880-016-0126-z.

[67] D. Kendoff, M. Citak, M. J. Gardner, T. Stübig, C. Krettek, and T. Hüfner, "Intraoperative 3D imaging: Value and consequences in 248 cases," *J. Trauma - Inj. Infect. Crit. Care*, vol. 66, no. 1, pp. 232–238, 2009, doi: 10.1097/TA.0b013e31815ede5d.

[68] G. Lekakis, P. Claes, G. S. Hamilton, and P. W. Hellings, "Three-Dimensional Surface Imaging and the Continuous Evolution of Preoperative and Postoperative Assessment in Rhinoplasty," *Facial Plast. Surg.*, vol. 32, no. 1, pp. 88–94, 2016, doi: 10.1055/s-0035-1570122.

[69] B. van Loon *et al.*, "3D Stereophotogrammetric assessment of pre- and postoperative volumetric changes in the cleft lip and palate nose," *Int. J. Oral Maxillofac. Surg.*, vol. 39, no. 6, pp. 534–540, 2010, doi: 10.1016/j.ijom.2010.03.022.

[70] I. Tulloch and J. S. Rubin, "Assessment and Management of Preoperative Anxiety," *J. Voice*, vol. 33, no. 5, pp. 691–696, 2019, doi: 10.1016/j.jvoice.2018.02.008.

[71] W. Jiang *et al.*, "Evaluation of the 3D Augmented Reality–Guided Intraoperative Positioning of Dental Implants in Edentulous Mandibular Models," *Int. J. Oral Maxillofac. Implants*, vol. 33, no. 6, pp. 1219–1228, 2018, doi: 10.11607/jomi.6638.

[72] G. J. C. van Baar, N. P. T. J. Liberton, H. A. H. Winters, L. Leeuwrik, T. Forouzanfar, and F. K. J. Leusink, "A postoperative evaluation guideline for computer-assisted reconstruction of the mandible," *J. Vis. Exp.*, vol. 2020, no. 155, pp. 1–9, 2020, doi: 10.3791/60363.

[73] S. Marbacher *et al.*, "Comparison of intra- And postoperative 3-dimensional digital subtraction angiography in evaluation of the surgical result after intracranial aneurysm treatment," *Neurosurgery*, vol. 87, no. 4, pp. 689–696, 2020, doi: 10.1093/neuros/nyz487.

[74] Y. Kim, K. Il Kim, J. H. Choi, and K. Lee, "Novel methods for 3D postoperative analysis of total knee arthroplasty using 2D-3D image

registration," *Clin. Biomech.*, vol. 26, no. 4, pp. 384–391, 2011, doi: 10.1016/j.clinbiomech.2010.11.013.

[75] M. Rana, N. C. Gellrich, U. Joos, J. Piffkó, and W. Kater, "3D evaluation of postoperative swelling using two different cooling methods following orthognathic surgery: A randomised observer blind prospective pilot study," *Int. J. Oral Maxillofac. Surg.*, vol. 40, no. 7, pp. 690–696, 2011, doi: 10.1016/j.ijom.2011.02.015.

[76] H. Imai, J. Miyawaki, T. Kamada, J. Takeba, N. Mashima, and H. Miura, "Preoperative planning and postoperative evaluation of total hip arthroplasty that takes combined anteversion," *Eur. J. Orthop. Surg. Traumatol.*, vol. 26, no. 5, pp. 493–500, 2016, doi: 10.1007/s00590-016-1777-8.

[77] G. J. C. van Baar, N. P. T. J. Liberton, T. Forouzanfar, H. A. H. Winters, and F. K. J. Leusink, "Accuracy of computer-assisted surgery in mandibular reconstruction: A postoperative evaluation guideline," *Oral Oncol.*, vol. 88, no. November 2018, pp. 1–8, 2019, doi: 10.1016/j.oraloncology.2018.11.013.

[78] G. Zheng, A. Alcoltekin, B. Thelen, and L. P. Nolte, "3X-knee: A novel technology for 3D preoperative planning and postoperative evaluation of TKA based on 2D X-rays," *Adv. Exp. Med. Biol.*, vol. 1093, pp. 93–103, 2018, doi: 10.1007/978-981-13-1396-7_8.

[79] J. Dubousset, B. Ilharreborde, and J. C. Le Huec, "Use of EOS imaging for the assessment of scoliosis deformities: Application to postoperative 3D quantitative analysis of the trunk," *Eur. Spine J.*, vol. 23, no. SUPPL. 4, 2014, doi: 10.1007/s00586-014-3334-7.

[80] A. Hanssen *et al.*, "3D Volumetry and its Correlation Between Postoperative Gastric Volume and Excess Weight Loss After Sleeve Gastrectomy," *Obes. Surg.*, vol. 28, no. 3, pp. 775–780, 2018, doi: 10.1007/s11695-017-2927-8.

[81] J. Borggrefe *et al.*, "Comparison of intraoperative flat panel imaging and postoperative plain radiography for the detection of intraarticular screw displacement in volar distal radius plate ostheosynthesis," *Orthop. Traumatol. Surg. Res.*, vol. 101, no. 8, pp. 913–917, 2015, doi: 10.1016/j.otsr.2015.07.023.

[82] N. H. Choi, S. J. Lee, S. C. Park, and B. N. Victoroff, "Comparison of Postoperative Tunnel Widening After Hamstring Anterior Cruciate Ligament Reconstructions Between Anatomic and Nonanatomic Femoral Tunnels," *Arthrosc. - J. Arthrosc. Relat. Surg.*, vol. 36, no. 4, pp. 1105–1111, 2020, doi: 10.1016/j.arthro.2019.10.021.

[83] H. Seok, S. G. Kim, Y. W. Park, and Y. C. Lee, "Postoperative three-dimensional evaluation of mandibular contouring surgery using computer-assisted simulation planning and a three-dimensional-printed surgical guide," *J. Craniofac. Surg.*, vol. 28, no. 3, pp. 768–770, 2017, doi: 10.1097/SCS.0000000000003442.

[84] A. Verhulst, M. Hol, R. Vreeken, A. Becking, D. Ulrich, and T. Maal, "Three-Dimensional Imaging of the Face: A Comparison between Three

Different Imaging Modalities," *Aesthetic Surg. J.*, vol. 38, no. 6, pp. 579–585, 2018, doi: 10.1093/asj/sjx227.

[85] K. Kimoto and N. R. Garrett, "Evaluation of a 3D digital photographic imaging system of the human face," *J. Oral Rehabil.*, vol. 34, no. 3, pp. 201–205, 2007, doi: 10.1111/j.1365-2842.2006.01663.x.

[86] J. Wu, R. Tse, and L. G. Shapiro, "Automated face extraction and normalization of 3D Mesh Data," *2014 36th Annu. Int. Conf. IEEE Eng. Med. Biol. Soc. EMBC 2014*, pp. 750–753, 2014, doi: 10.1109/EMBC.2014.6943699.

[87] U. Hanaoka, H. Tanaka, K. Koyano, R. Uematsu, K. Kanenishi, and T. Hata, "HDlive imaging of the face of fetuses with autosomal trisomies," *J. Med. Ultrason.*, vol. 41, no. 3, pp. 339–342, 2014, doi: 10.1007/s10396-014-0523-2.

[88] T. J. J. Maal *et al.*, "Variation of the face in rest using 3D stereophotogrammetry," *Int. J. Oral Maxillofac. Surg.*, vol. 40, no. 11, pp. 1252–1257, 2011, doi: 10.1016/j.ijom.2011.02.033.

[89] K. C. Koban *et al.*, "Precision in 3-Dimensional Surface Imaging of the Face: A Handheld Scanner Comparison Performed in a Cadaveric Model," *Aesthetic Surg. J.*, vol. 39, no. 4, pp. NP36–NP44, 2019, doi: 10.1093/asj/sjy242.

[90] R. Sawh-Martinez and D. M. Steinbacher, "Commentary on: Three-Dimensional Imaging of the Face: A Comparison between Three Different Imaging Modalities," *Aesthetic Surg. J.*, vol. 38, no. 6, pp. 586–589, 2018, doi: 10.1093/asj/sjy025.

[91] K. C. Koban, S. Leitsch, T. Holzbach, E. Volkmer, P. M. Metz, and R. E. Giunta, "3D Bilderfassung und Analyse in der Plastischen Chirurgie mit Smartphone und Tablet: eine Alternative zu professionellen Systemen?," *Handchirurgie Mikrochirurgie Plast. Chir.*, vol. 46, no. 2, pp. 97–104, 2014, doi: 10.1055/s-0034-1371822.

[92] T. Oliveira-Santos *et al.*, "3D face reconstruction from 2D pictures: First results of a web-based computer aided system for aesthetic procedures," *Ann. Biomed. Eng.*, vol. 41, no. 5, pp. 952–966, 2013, doi: 10.1007/s10439-013-0744-3.

[93] M. R. Markiewicz and R. B. Bell, "The Use of 3D Imaging Tools in Facial Plastic Surgery," *Facial Plast. Surg. Clin. North Am.*, vol. 19, no. 4, pp. 655–682, 2011, doi: 10.1016/j.fsc.2011.07.009.

[94] S. Tulyakov, L. A. Jeni, J. F. Cohn, and N. Sebe, "Viewpoint-Consistent 3D Face Alignment," *IEEE Trans. Pattern Anal. Mach. Intell.*, vol. 40, no. 9, pp. 2250–2264, 2018, doi: 10.1109/TPAMI.2017.2750687.

[95] J. D. White *et al.*, "Sources of variation in the 3dMDface and Vectra H1 3D facial imaging systems," *Sci. Rep.*, vol. 10, no. 1, pp. 1–10, 2020, doi: 10.1038/s41598-020-61333-3.

[96] J. Pallanch, "Introduction to 3D Imaging Technologies for the Facial Plastic Surgeon," *Facial Plast. Surg. Clin. North Am.*, vol. 19, no. 4, pp. xv–xvi, 2011, doi: 10.1016/j.fsc.2011.07.001.

[97] R. Nedelcu, P. Olsson, I. Nyström, and A. Thor, “Finish line distinctness and accuracy in 7.pdf,” pp. 1–11, 2018.

[98] C. M. Oranges *et al.*, “Three-dimensional Assessment of the Breast: Validation of a novel, simple and inexpensive scanning process,” *In Vivo (Brooklyn).*, vol. 33, no. 3, pp. 839–842, 2019, doi: 10.21873/invivo.11548.

[99] R. Nedelcu, P. Olsson, I. Nyström, J. Rydén, and A. Thor, “Accuracy and precision of 3 intraoral scanners and accuracy of conventional impressions: A novel in vivo analysis method,” *J. Dent.*, vol. 69, pp. 110–118, 2018, doi: 10.1016/j.jdent.2017.12.006.

[100] J. Jin *et al.*, “3-D wound scanner: A novel, effective, reliable, and convenient tool for measuring scar area,” *Burns*, vol. 44, no. 8, pp. 1930–1939, 2018, doi: 10.1016/j.burns.2018.05.009.

[101] S. Shah, G. Sundaram, D. Bartlett, and M. Sherriff, “The use of a 3D laser scanner using superimpositional software to assess the accuracy of impression techniques,” *J. Dent.*, vol. 32, no. 8, pp. 653–658, 2004, doi: 10.1016/j.jdent.2004.07.005.

[102] K. W. Lee, S. H. Kim, Y. C. Gil, K. S. Hu, and H. J. Kim, “Validity and reliability of a structured-light 3D scanner and an ultrasound imaging system for measurements of facial skin thickness,” *Clin. Anat.*, vol. 30, no. 7, pp. 878–886, 2017, doi: 10.1002/ca.22931.

[103] P. G. M. Knoops *et al.*, “Comparison of three-dimensional scanner systems for craniomaxillofacial imaging,” *J. Plast. Reconstr. Aesthetic Surg.*, vol. 70, no. 4, pp. 441–449, 2017, doi: 10.1016/j.bjps.2016.12.015.

[104] H. L. Rudy, N. Wake, J. Yee, E. S. Garfein, and O. M. Tepper, “Three-Dimensional Facial Scanning at the Fingertips of Patients and Surgeons: Accuracy and Precision Testing of iPhone X Three-Dimensional Scanner,” *Plast. Reconstr. Surg.*, pp. 1407–1417, 2020, doi: 10.1097/PRS.0000000000007387.

[105] L. Kovacs *et al.*, “Three-dimensional recording of the human face with a 3D laser scanner,” *J. Plast. Reconstr. Aesthetic Surg.*, vol. 59, no. 11, pp. 1193–1202, 2006, doi: 10.1016/j.bjps.2005.10.025.

[106] T. Kihara, Y. Yoshimi, T. Taji, T. Murayama, K. Tanimoto, and H. Nikawa, “Accuracy of a three-dimensional dentition model digitized from an interocclusal record using a non-contact surface scanner,” *Eur. J. Orthod.*, vol. 38, no. 4, pp. 435–439, 2016, doi: 10.1093/ejo/cjv065.

[107] L. Sennerby *et al.*, “Evaluation of a Novel Cone Beam Computed Tomography Scanner for Bone Density Examinations in Preoperative 3D Reconstructions and Correlation with Primary Implant Stability,” *Clin. Implant Dent. Relat. Res.*, vol. 17, no. 5, pp. 844–853, 2015, doi: 10.1111/cid.12193.

[108] P. Medina-Sotomayor, A. Pascual-Moscardó, and I. Camps, “Correction: Accuracy of four digital scanners according to scanning strategy in completearch impressions (PLoS ONE (2018) 13:9 (e0202916) DOI: 10.1371/journal.pone.0202916),” *PLoS One*, vol. 13, no. 12, pp. 1–14, 2018, doi: 10.1371/journal.pone.0209883.

[109] K. C. Koban, F. Härtnagl, V. Titze, T. L. Schenck, and R. E. Giunta, “Chances and limitations of a low-cost mobile 3D scanner for breast imaging in comparison to an established 3D photogrammetric system,” *J. Plast. Reconstr. Aesthetic Surg.*, vol. 71, no. 10, pp. 1417–1423, 2018, doi: 10.1016/j.bjps.2018.05.017.

Acknowledgements

When I began to write my thesis, I was in a very excited and scared mood. What excited me was that I was about to face the final stage of my doctoral study, and what scared me was that I might not be able to write this significant doctoral thesis well. Fortunately, with the help of many teachers and colleagues, I successfully completed my doctoral thesis.

First, I would like to thank my three supervisors, Prof. Dr. Med. Thilo Ludwig Schenck, Prof. Dr. Med. Riccardo Enzo Giunta, Prof. Dr. Med. Sebastian Cotofana.I thank them for their guidance on my project during my doctoral study.

Secondly, I would like to thank my two co-supervisors, Dr. Med. Konstantin Frank and Dr. Med. Konstantin Koban. Both of them have helped me a lot in my MD project and in my daily life in Munich. I think our daily relationship mode is not so much teachers and students as friends.

Then I would like to thank the Ludwig-Maximilians-University for providing me with a great place and opportunity to study. During my three years in Munich, I have made many friends and classmates, and we have helped and learned from each other. These have been three happy years of my life. Thanks again to the Ludwig-Maximilians-University.

Finally, I would like to thank all my colleagues in the Department of Plastic Surgery at the University Hospital of Munich. They help me a lot in my daily life and work and treat me like friend. I am happy to work with them. I hope I can study here again if I have a chance in the future.

Thanks again to my teachers, colleagues and classmates. Thank you.

Affidavit

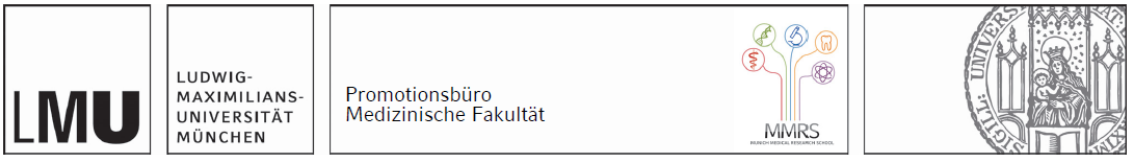

Affidavit

Xu Ya
_____
Surname, first name

_____
Street

_____
Zip code, town, country

I hereby declare, that the submitted thesis entitled:

Reliability and Comparison of 3-Dimensional Surface Imaging of the Face Using a Hand-Held and Whole body Surface Scanner

……

is my own work. I have only used the sources indicated and have not made unauthorised use of services of a third party. Where the work of others has been quoted or reproduced, the source is always given.

I further declare that the submitted thesis or parts thereof have not been presented as part of an examination degree to any other university.

Munich 28,03,2022 Ya Xu
_____
_____
place date Signature doctoral candidate

List of publications

1. Xu Y, Frank K, Kohler L, Ehrl D, Alfertshofer M, Giunta RE, Moellhoff N, Cotofana S, Koban KC. Reliability of 3-dimensional surface imaging of the face using a whole-body surface scanner. J Cosmet Dermatol. 2021 Nov 3. doi: 10.1111/jocd.14555. Epub ahead of print. PMID: 34731521.

2. Etzel L, Schenck TL, Giunta RE, Li Z, Xu Y, Koban KC. Digital Leg Volume Quantification: Precision Assessment of a Novel Workflow Based on Single Capture Three-dimensional Whole-Body Surface Imaging. J Digit Imaging. 2021 Oct;34(5):1171-1182. doi: 10.1007/s10278-021-00493-8. Epub 2021 Sep 28. PMID: 34581929; PMCID: PMC8554908.